Naval-108

NAVAL POSTGRADUATE SCHOOL
Monterey, California

THESIS

INVESTIGATION OF HEAT TRANSFER IN STRAIGHT AND CURVED RECTANGULAR DUCTS

by

James Claude Ballard, III

September 1980

Thesis Advisor: M. Kelleher

Approved for public release; distribution unlimited

SECURITY CLASSIFICATION OF THIS PAGE (When Data Entered)

REPORT DOCUMENTATION PAGE

READ INSTRUCTIONS BEFORE COMPLETING FORM

1. REPORT NUMBER	2. GOVT ACCESSION NO. / 3. RECIPIENT'S CATALOG NUMBER
4. TITLE (and Subtitle): Investigation of Heat Transfer in Straight and Curved Rectangular Ducts	5. TYPE OF REPORT & PERIOD COVERED: Master's Thesis; September 1980
	6. PERFORMING ORG. REPORT NUMBER
7. AUTHOR(s): James Claude Ballard, III	8. CONTRACT OR GRANT NUMBER(s)
9. PERFORMING ORGANIZATION NAME AND ADDRESS: Naval Postgraduate School, Monterey, California 93940	10. PROGRAM ELEMENT, PROJECT, TASK AREA & WORK UNIT NUMBERS
11. CONTROLLING OFFICE NAME AND ADDRESS: Naval Postgraduate School, Monterey, California 93940	12. REPORT DATE: September 1980
	13. NUMBER OF PAGES: 71
14. MONITORING AGENCY NAME & ADDRESS(if different from Controlling Office)	15. SECURITY CLASS. (of this report): UNCLASSIFIED
	15a. DECLASSIFICATION/DOWNGRADING SCHEDULE

16. DISTRIBUTION STATEMENT (of this Report)

Approved for Public Release; distribution unlimited

17. DISTRIBUTION STATEMENT (of the abstract entered in Block 20, if different from Report)

18. SUPPLEMENTARY NOTES

19. KEY WORDS (Continue on reverse side if necessary and identify by block number)

Taylor-Görtler Vortices, Heat Transfer, Rectangular Curved Channel, Rectangular Straight Channel, Temsheet, Liquid Crystals

20. ABSTRACT (Continue on reverse side if necessary and identify by block number)

Experimental investigations have been conducted to examine the general problem of convective heat transfer in a rectangular cross section channel with both straight and curved passages. The experimental configuration was modeled as infinite parallel plates with one wall at a constant heat flux and the opposite wall adiabatic. The air flow through the channel was heated through the Joulean heating of a wall composed of Temsheet. Liquid crystals applied to

DD FORM 1 JAN 73 1473 (Page 1) EDITION OF 1 NOV 65 IS OBSOLETE S/N 0102-014-6601

SECURITY CLASSIFICATION OF THIS PAGE (When Data Entered)

the surface of the Temsheet were used to confirm the presence of the Taylor-Görtler vortices. Average Nusselt number measurements were used to investigate their effect on heat transfer from the curved test section. Experiments were conducted for steady state laminar flow that was hydrodynamically developed and thermally developing. It was confirmed that the Taylor-Görtler vortices enhanced the heat transfer process in the curved section. The experimental data was compared with several analytic studies with good results

Approved for Public Release; distribution unlimited

Investigation of Heat Transfer in Straight and Curved Rectangular Ducts

by

James Claude Ballard, III
Lieutenant, United States Navy
B.S.M.E., Rensselaer Polytechnic Institute, 1973

Submitted in partial fulfillment of the requirement
for the degree of

MASTER OF SCIENCE IN MECHANICAL ENGINEERING

from the

NAVAL POSTGRADUATE SCHOOL
September 1980

ABSTRACT

Experimental investigations have been conducted to examine the general problem of convective heat transfer in a rectangular cross section channel with both straight and curved passages. The experimental configuration was modeled as infinite parallel plates with one wall at a constant heat flux and the opposite wall adiabatic. The air flow through the channel was heated through the Joulean heating of a wall composed of Temsheet. Liquid crystals applied to the surface of the Temsheet were used to confirm the presence of the Taylor-Görtler vortices. Average Nusselt number measurements were used to investigate their effect on heat transfer from the curved test section. Experiments were conducted for steady state laminar flow that was hydrodynamically developed and thermally developing. It was confirmed that the Taylor-Görtler vortices enhanced the heat transfer process in the curved section. The experimental data was compared with several analytic studies with good results.

TABLE OF CONTENTS

LIST OF TABLES

LIST OF FIGURES

TABLE OF SYMBOLS

Symbol	Meaning	Units
A_c	cross sectional area of the channel	m^2
A_{PL}	area of the wall heater (Temsheet)	m^2
C_{Pair}	specific heat of air at constant pressure	KJ/Kg °C
d	height of the channel	m
De	Dean number	
Dh	hydraulic diameter	m
F_{wo-wi}	radiation shape factor	
$\bar{h}$	average heat transfer coefficient	W/m^2 °C
K_{air}	thermal conductivity of air	W/m °C
K_{INS}	thermal conductivity of insulation	W/m °C
$\dot{m}$	mass flow rate of air	Kg/sec
Nu	local Nusselt number	
$\overline{Nu}$	average Nusselt number	
$\overline{Nu}_c$	average Nusselt number in curved section	
$\overline{Nu}_s$	average Nusselt number in straight section	
Pr	Prandtl number	
p	atmospheric pressure	N/m^2
Q	rotameter flow percentage	
$\dot{q}$	volumetric flow rate of air	m^3/sec
Qair	heat convected to the air	W
Q_{Li}	heat lost through inner wall(Plexiglass)	W
Q_{Lo}	heat lost through outer wall(Temsheet)	W
Q_p	power supplied	

Symbol	Meaning	Units
Q_r	heat transferred by radiation	W
Q_{wi}	heat transferred from the inner wall	W
Q_{wo}	heat transferred from the outer wall	W
R	gas constant for air	J/Kg °K
Re	Reynolds number	
Ri	radius of curvature of inner wall	m
R_{PR}	electrical resistance of precision resistor	Ω
R_R	total radiation resistance	m^{-2}
Ta	Taylor number	
T_B	bulk temperature of the flow	°C
T_{EXIT}	flow exit temperature	°C
T_{IN}	average flow inlet temperature	°C
T_{INS}	temperature of the insulation	°C
T_{ROOM}	ambient temperature	°C
T_{OUT}	average flow outlet temperature after each test section	°C
T_{wi}	average temperature of inner wall	°K
T_{wo}	average temperature of outer wall	°K
V_{PR}	voltage across precision resistor	V
V_H	voltage across wall heater(Temsheet)	V
x*	dimensionless axial length coordinate	
ε_{wi}	emissivity of inner wall (Plexiglas)	
ε_{wo}	emissivity of outer wall (Temsheet)	
Θ	temperature correction to standard conditions	

Symbol	Meaning	Units
μ_{air}	dynamic viscosity of air	Kg/m·sec
ρ	density of air	Kg/m^3
σ	Stefan - Boltzmann constant	$W/m^2{}^\circ K$
ΔT	mean temperature difference	°C
ΔT_{INS}	temperature difference in insulation	°C
ΔX_{INS}	thickness of insulation layers	m

ACKNOWLEDGMENT

It is very seldom that the development and completion of a project of this nature can be attributed to a single person alone, and this study is no exception. The author wishes to express his sincere appreciation to Professor Matthew D. Kelleher for his valuable advice and guidance throughout the term of this project. Without his tireless assistance and direction this thesis would have been a nearly insurmountable task.

In addition the personnel of the Mechanical Engineering Shop deserve a special thanks for their assistance and skill in construction and preparation of the experimental apparatus.

Finally, the author wishes to thank his wife Andrea for her understanding and encouragement throughout the entire course of this study.

I. INTRODUCTION

A. DESCRIPTION OF TAYLOR-GÖRTLER VORTICES

A considerable amount of data and indirect evidence, [1, 2, 3] among others, has shown that the fully developed laminar flow of viscous fluids along a concave wall does not remain two dimensional. Instead, the flow forms spiral vortices in counter-rotating pairs which frequently possess a regularly spaced cellular structure. This phenomenon, known as Taylor-Görtler vortices, occurs as a result of flow instability induced by variations in the centrifugal forces acting on fluid particles. The Taylor-Görtler vortices are laminar in nature with their axes aligned in the direction of the principal fluid flow and with secondary flow velocities in both perpendicular directions. An example of this flow pattern is shown in Figure 1.

In a channel that is curved in the streamwise direction, such as that used in this study, the fluid particles near the center are subjected to higher centrifugal forces than those experienced by the slower moving fluid particles near the boundary of the concave wall. Consequently, the tendency is for the fluid particles in the center of the channel to move outward to the concave wall. Under this influence, particles near the wall are displaced initially in the spanwise direction and subsequently continue radially inward,

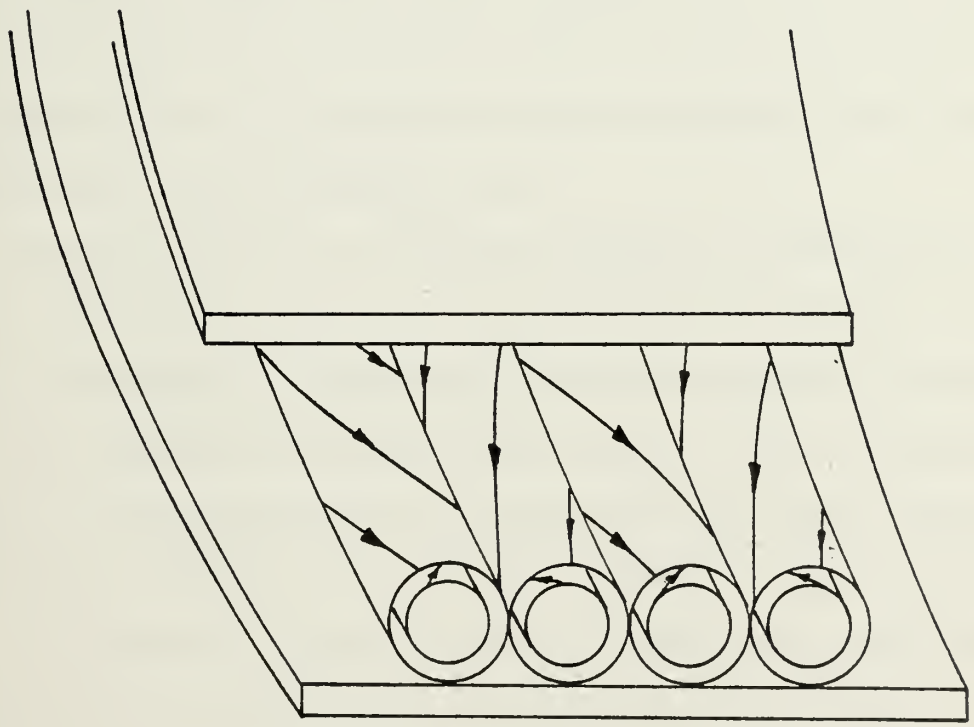

Figure 1. Taylor-Görtler Vortex Flow Pattern

replacing the central fluid particles. Once in the center of the channel the fluid particle will come under the influence of the higher free stream velocity and resultant centrifugal forces. This action forces movement back toward the concave wall causing the entire cyclic rotation process to propagate.

Although the Taylor-Görtler vortices are laminar, it is quite possible that they play an important role in the transition from the laminar to the turbulent flow regime. [2] Additionally, the presence of the vortices have been thought to account for the increase in heat transfer from curved walls due to mass transfer. [4]

The Taylor-Görtler vortices also have similarities to other vortex flow patterns such as the longitudinal vortex rolls developed in the laminar forced convection heating of fluid layers between parallel plates. [5] In another field it has further been hypothesized that the cross-hatching phenomenon observed in re-entry vehicles can be explained by the presence of centrifugally induced secondary motion characteristic of the Taylor-Görtler vortices. [6]

It is apparent that the understanding of these vortices and their effect on heat transfer and fluid flow characteristics could significantly effect many areas of fluid mechanics. Recently it has been proposed [7, 8, 9] that concave wall curvature can have an advantageous effect on film cooling over turbine blades.

Many applications of fluid mechanics and heat transfer involve curved surfaces or curved channels and the understanding of the fluid mechanics in this geometry will greatly enhance engineering designs and capabilities.

B. BRIEF HISTORY

Instability of an inviscid fluid in a curved flow was first considered by Lord Raleigh in 1916. [10] He concluded that the stability criterion for an inviscid fluid had as a necessary condition that the circulation always increased with the radius. In essence, this meant that the product of the local circumferential velocity and the corresponding local radius of curvature cannot decrease with increasing radial distance.

In 1923, G. I. Taylor expanded the scope of Raleigh's stability criterion to include viscous fluids. [1, 11] His extensive analytic and experimental investigation focused on the flow of viscous fluids between a rotating inner cylinder and a stationary outer cylinder. Taylor ascertained that such couette flows become unstable when a characteristic, non-dimensional parameter exceeded a critical value of 41. Referred to as the Taylor number, this parameter was defined as:

$$Ta = \frac{Ud}{\nu}\sqrt{\frac{d}{R_i}} = Re\sqrt{\frac{d}{R_i}}$$

In this relationship d represents the spacing between the concentric cylinders, assumed small when compared to the radius of curvature, R_i. Re is the Reynolds number based on U, the circumferential velocity of the inner cylinder and d, the annulus width. When flow conditions were such that the Taylor number exceeded this critical value, the secondary flow observed in the gap between the stationary outer cylinder and the concentrically rotating inner cylinder was in the form of longitudinal vortices whose axes were aligned in the circumferential direction. These vortices were given the name Taylor vortices.

A similar form of instability occurs when a viscous fluid flows in a curved channel due to a pressure gradient acting along the concave wall. W. R. Dean [12] first addressed this problem analytically in 1928. Specifically, he considered flow in a channel formed by two concentric cylinders with the restriction that the cylinder gap distance be small compared to the radius of the inner cylinder. Dean concluded that the flow instability would initiate, and the secondary flow vortices (similar to the Taylor vortices) would form, when the Dean number was greater than 36. The Dean number was then defined as:

$$De = Re \sqrt{\frac{d}{Ri}}$$

In this case, the Reynolds number was based on the mean velocity of the undisturbed flow and d represented the channel half width. The analytical work by Dean was later verified by W. H. Reid [13] using an approximate numerical solution.

In 1940, H. Görtler [2] studied the influence of small disturbances on the stability of laminar boundary layer profiles. Görtler found that these disturbances closely resembled those described by G. I. Taylor which led to fluid flow instability in the form of vortices. In his numerical calculations, Görtler concluded that the amplified disturbances were produced only on the concave walls; nonetheless, the overall flow regime seemed to remain laminar. The approximate analytic results that Görtler had developed were initially verified with an exact solution by G. Hammerlin as reported by H. Schlicting [14], and later substantiated by an extensive numerical analysis by A. M. O. Smith [3]. M. Kelleher, et al., [15] and S. Winoto, et al., [16], among others, have been able to verify these numerical predictions by using hot wire anemometry, laser Doppler systems and flow visualization techniques to describe the motion of the secondary flow. A non-linear analysis of Görtler vortices was conducted by Y. Aihara [17] in 1976.

Growing interest in the various effects of the secondary flow associated with Taylor-Görtler vortices led to more specific studies concerning the vortice influence on heat transfer in both turbulent and laminar flow. In 1955,

F. Kreith [4] reported that the heat transfer from a heated concave wall was considerably higher than that from a convex wall of identical curvature under similar conditions of turbulent flow.

In the special cases of very high or very low Prandtl number, L. Persen [18] related the increased heat transfer from curved walls to the presence of Taylor-Görtler vortices. He determined that their overall effect was to enhance heat transfer through the boundary layer.

In 1970, McCormack, et al., [19] published the results of their initial experimental work regarding the effect of secondary flow on heat transfer. From the data obtained they concluded that a complete theoretical explanation of the heat transfer effects required that all non-linear terms be retained in the flow equations. R. Kahawita and R. Meroney [20] considered this hypothesis and further reported that both the high order terms and the normal velocity components of the main flow were essential to any calculations at small wave numbers.

In 1966, Y. Mori and Y. Uchida [5] considered the fully developed forced convection heat transfer between horizontal plates. In the results of their investigation they reported that as the temperature difference between the plates was increased a critical value developed beyond which longitudinal vortex rolls, similar to the Taylor-Görtler vortices, would

form with their axes in the streamwise direction. M. Akiyama, et al., [21] confirmed the presence of these longitudinal vortices at a critical Rayleigh number of 1708 in cases where the plate is heated from below.

Although heat transfer in curved duct flow has, and will continue to be investigated experimentally, considerable emphasis has been directed recently towards heat transfer predictions using numerical approximation for flows in curved duct geometries. In 1970, K. Cheng and M. Akiyama [22] developed a numerical solution for forced convection heat transfer in laminar curved rectangular channels by using a point successive over-relaxation method. For similar flow and boundary conditions, G. Yee and J. A. C. Humphrey [23] used the fully elliptic forms of the transport equations to compose a numerical solution. However, both of these numerical solutions were limited to small aspect ratios of essentially square cross section.

In contrast to the large volume of published numerical approximations to this heat transfer problem, the number of experimental and analytical investigations have been very limited. Results for a fully developed, constant wall heat flux, curved, square cross section channel were reported by Y. Mori, et al. [24], and results for larger aspect ratios were reported by M. Durao. [25]

II. INTENT OF THE STUDY

In view of the possible engineering design implications of the Taylor-Görtler vortex phenomenon, the primary purpose of this study was to investigate the effects of the secondary flow on the heat transfer rates in a curved channel of rectangular cross section.

It was expected that the presence of the Taylor-Görtler vortices would result in the secondary flow velocity components transporting the heated fluid particle from the curved wall to the center of the flow channel. This fluid motion would displace the cooler fluid particle in the center of the channel causing it to move toward the heated curved wall. It was anticipated that this cyclic motion would measurably improve the heat transfer process for all fluid velocities in the laminar flow regime. Secondary investigations were conducted to determine the additional influence of buoyant effects on the development of heat transfer in the curved channel. It was expected that the heat transfer rates would be greater when the buoyant forces were in the direction of the main flow.

The investigation was conducted using a rectangular cross section channel that contained both a straight and a curved test section. The results obtained in the straight

section served as a baseline and as such were compared to the data obtained in the curved section. The complete process was accomplished for two distinct channel orientations: (1) buoyant forces aligned with, and (2) buoyant forces opposed to, the main direction of the fluid flow.

Straight section data were compared with analytic solutions provided by P. McCuen, et al., [26], P. M. Worsøe-Schmidt [27] and R. K. Shah and A. L. London. [28] The buoyant effects were qualitatively compared with the data contained in a numerical computation by R. Chilukuri and J. A. C. Humphrey. [29]

III. EXPERIMENTAL WORK

A. DESCRIPTION OF THE APPARATUS

A rectangular cross section channel built as described in reference 25 was used to achieve the objectives of this study. The channel was manufactured from two 0.635 cm thick sheets of Plexiglas separated by 0.635 cm thick spacers whose inside lengths served as the sides of the channel.

As shown in Figure 2, the channel was composed of a straight portion 122.0 cm long, an intermediate curved section which formed a 180 degree arc and a final short straight section. The radius of curvature of the interior concave wall of the curved portion was 30.5 cm. The channel was 0.635 cm high and 25.4 cm wide with an aspect ratio of 40 and a cross sectional area of 16.13 square centimeters. A cross sectional view of the channel is shown in Figure 3.

The working fluid was air at room temperature which entered the flow channel through an entrance bell constructed of Plexiglas. The entrance bell was designed and manufactured in accordance with ASME nozzle standards with an elliptic curve based on a ten inch major and one inch minor axis. A permeable cloth covered the entrance nozzle to reduce the introduction of dust and other foreign matter into the flow channel. The flow at the end of the channel exited through

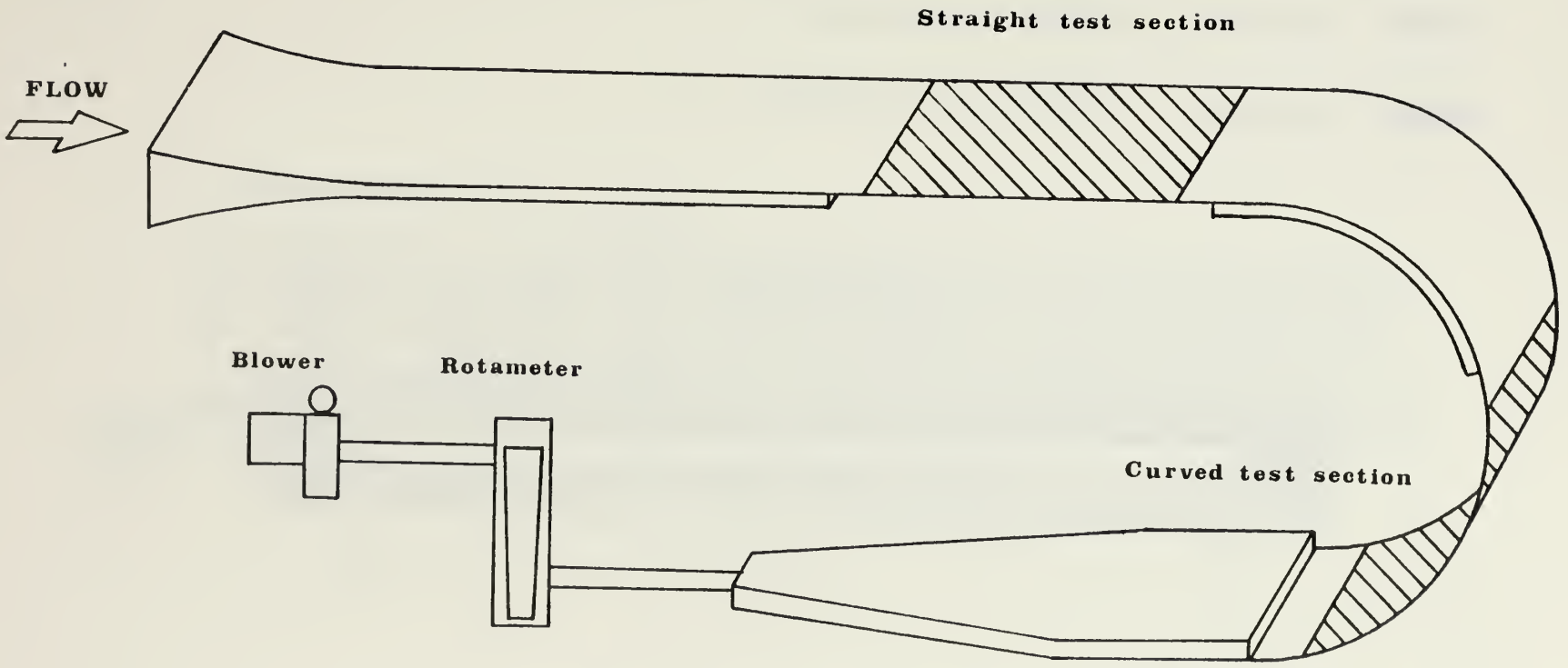

Figure 2. Schematic Illustration of Apparatus

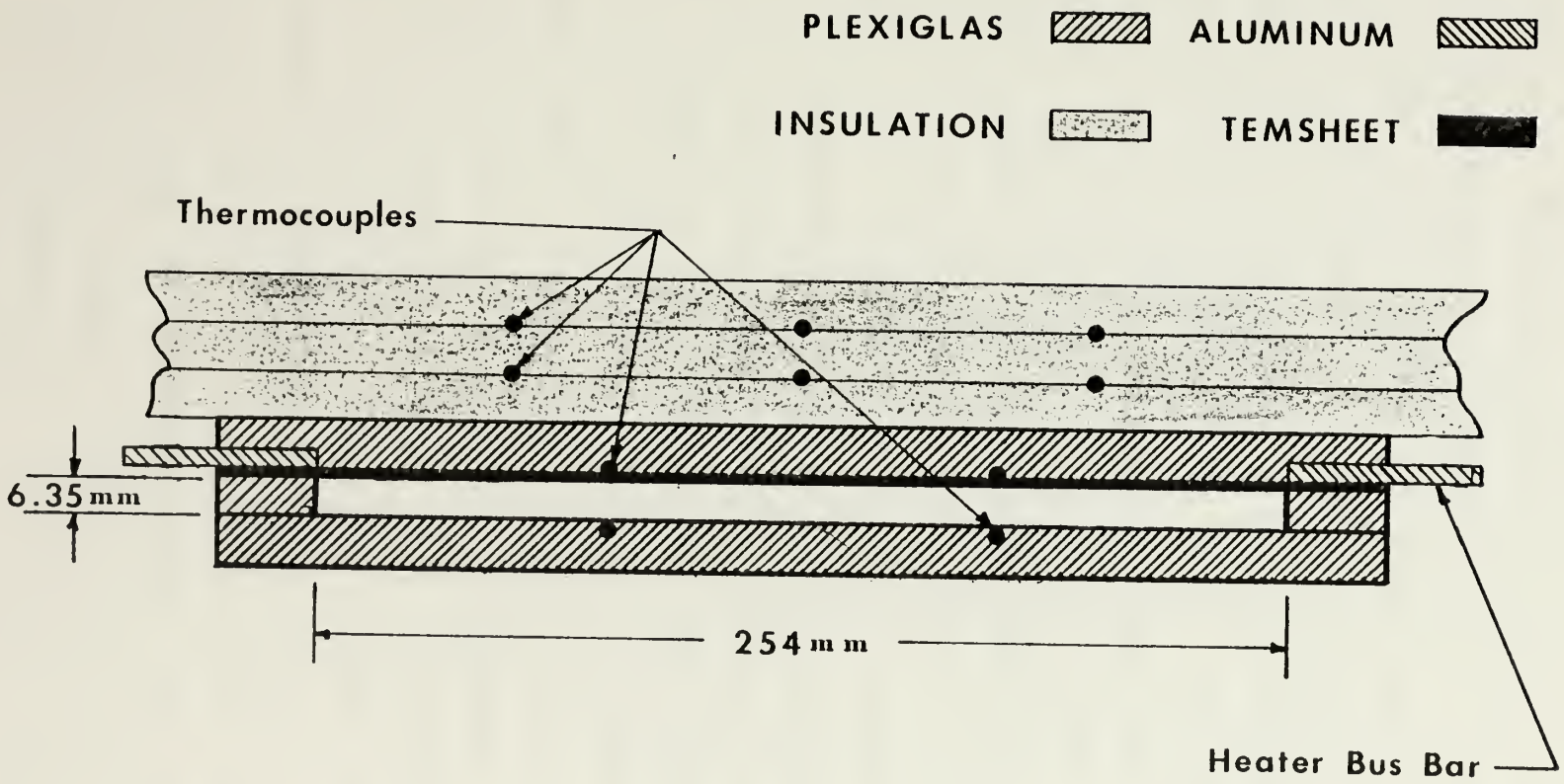

Figure 3. Cross Section of Channel at Both Test Sections

an aluminum exhaust bell connected by flexible tubing to a Fisher and Porter Company variable area flow meter, model number 10A3565A. The rotameter had a 100% full scale rating of 0.314 cubic meters of air per minute (11.1 standard cubic feet of air per minute) at one atmosphere and 70° F.

The flow of air was drawn through the channel, the flexible tubing and the rotameter by a single electrically driven, Cadillac centrifugal blower, model G-12. The blower speed was controlled by varying the motor voltage with a General Radio Company Variac Autotransformer type W10MT3.

For the purpose of obtaining experimental heat transfer data, two test sections were constructed; (1) a straight test section, 29.2 cm in length, located in the straight portion of the channel downstream of the hydrodynamic entrance region, and (2) a curved test section 28.3 cm in length, subtending a circular arc of 53.1° in the lower quadrant of the curved portion of the channel. The area of the straight test section was 741.9 square centimeters and that of the curved test section was 717.7 square centimeters.

In each test section the outer wall was detached and modified as shown in Figures 4 and 5. Temsheet, which is a carbon impregnated porous paper with the property of uniform electrical resistivity, was glued to the entire interior surface of the outer wall in each section. The flow of air could then be heated through the Joulean heating of the Temsheet. Since the Temsheet had an electrical resistance that

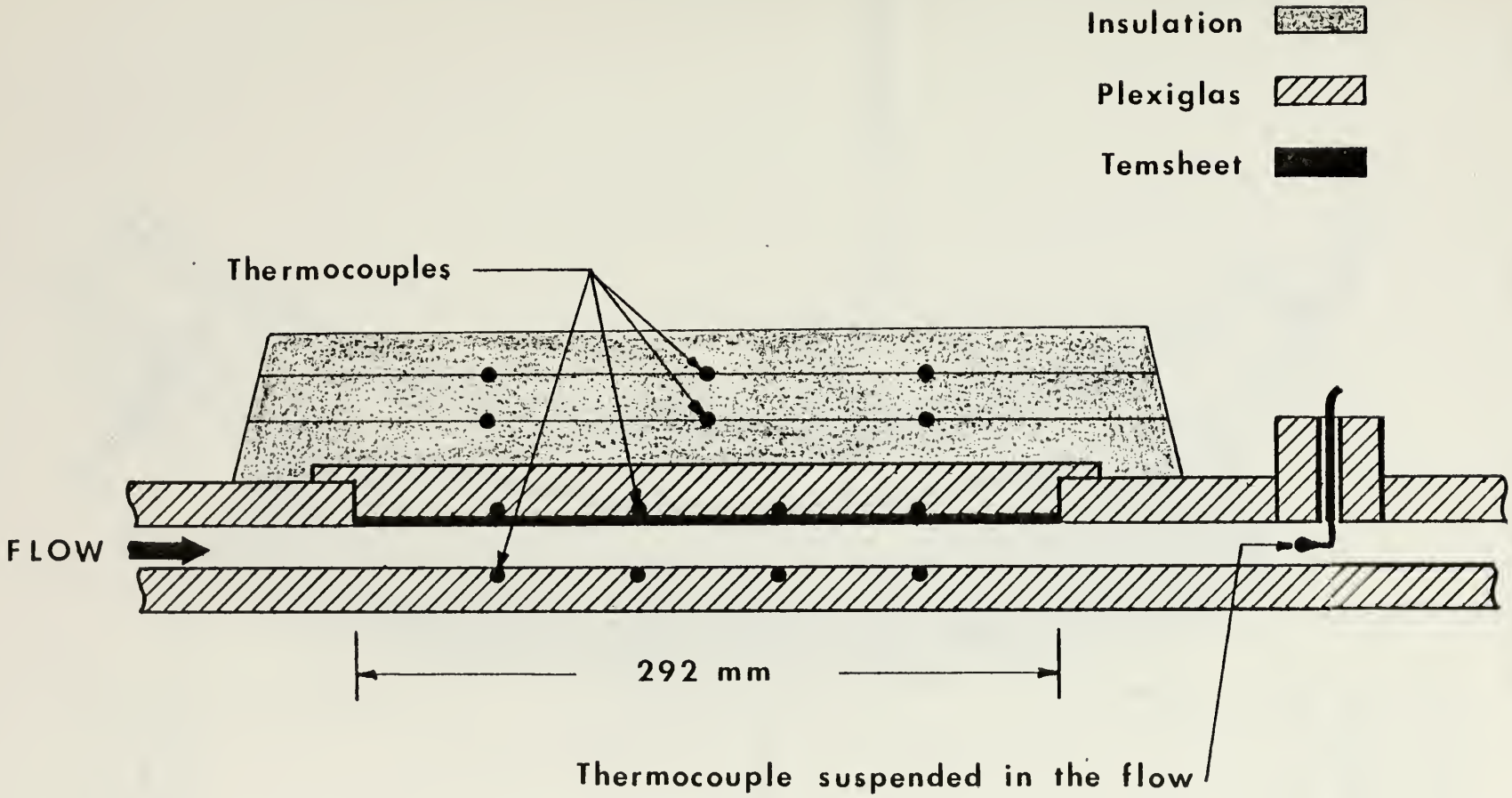

Figure 4. Internal Detail of the Straight Test Section

Figure 5. Internal Detail of the Curved Test Section

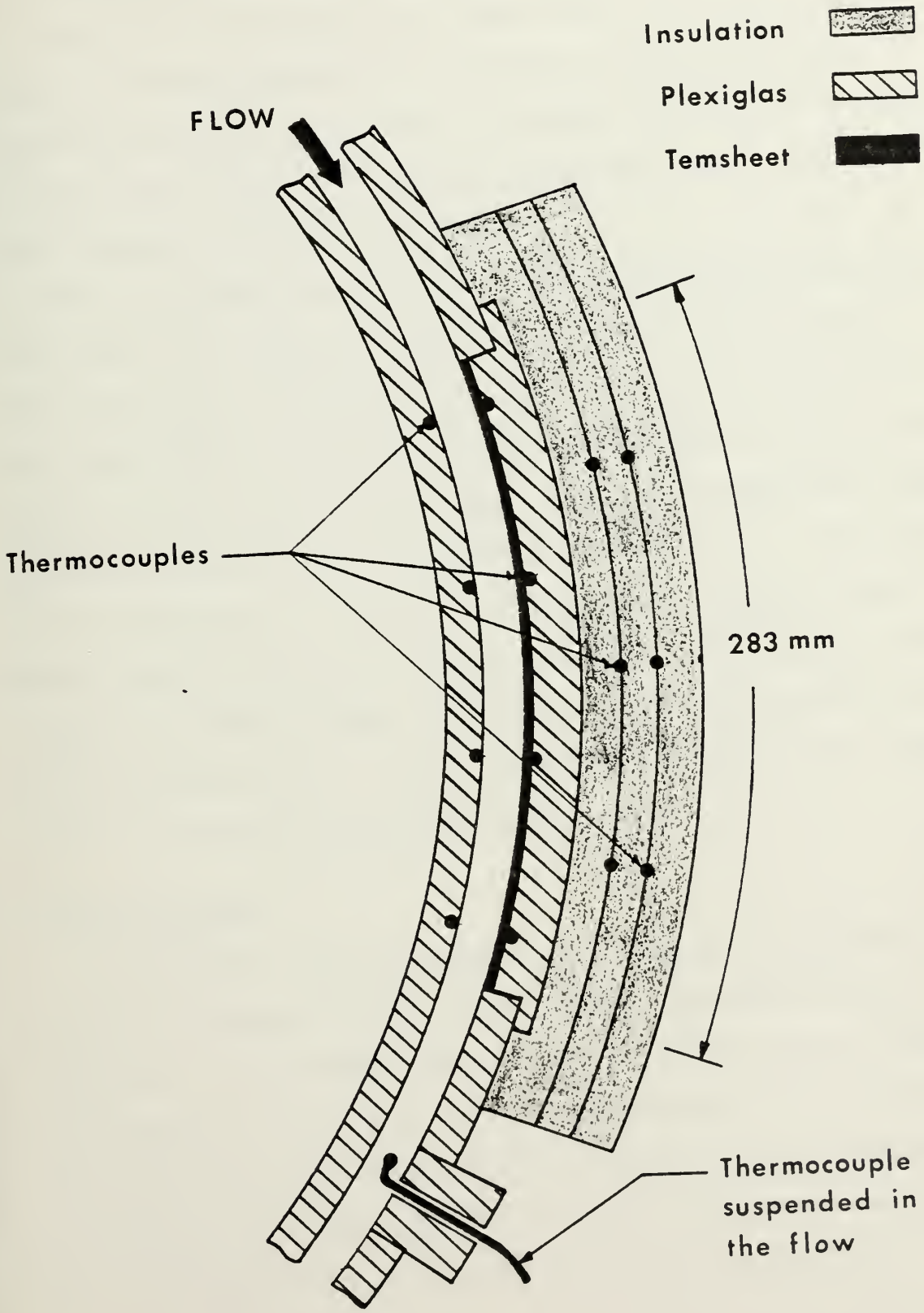

was slightly temperature dependent, a precision resistor with an electrical resistance of 2.0236 ohms was connected in series with the Temsheet to facilitate calculating the instantaneous power supplied. A LAMBDA Regulated D.C. Power Supply model LK345A FM supplied electrical current to heat the Temsheet to desired levels.

The variables to be measured in the investigation were: the flow inlet temperature at the entrance to each test section (T_{IN}), the flow outlet temperature at the exit of each test section (T_{OUT}), the wall temperature of the heated plate in each test section (T_{wo}), the wall temperature opposite the heated plate in each test section (T_{wi}), the flow exit temperature at the end of the channel (T_{EXIT}), the temperatures between the two insulation layers for each test section (T_{INS}), and the voltages across the precision resistor (V_{PR}) and the heater (V_H). Copper-Constantan thermocouples were used to measure all the above temperatures.

Liquid Crystals

Cholesteric Liquid Crystals were employed to provide qualitative measurements of the surface temperature distribution on the Temsheet. The liquid crystals exhibit dramatic changes in color for a small temperature differential. The liquid crystals would allow a reasonable qualitative comparison to be made between the heat transfer processes on each test section by observation of the color pattern

displayed for various temperature gradients and flow velocities. Specifically, the occurrence of multi-color stripes aligned in the flow direction on the curved wall would indicate regions of high and low temperatures and confirm the presence of Taylor-Görtler vortices.

To select the appropriate liquid crystal system for application to the surface of the Temsheet, consistent values of flow inlet temperature, Reynolds number, Prandtl number and Nusselt number were assumed and an approximate energy balance was developed:

$$Q = \dot{m}\, C_{pair}(T_{OUT} - T_{IN}) = \bar{h}\, A_{PL}\, \Delta T$$

or

$$\frac{\Delta T}{T_{OUT} - T_{IN}} = \frac{Re\ Pr}{Nu} \quad \frac{(A_c)}{(A_{PL})}$$

where

$$\Delta T = T_{wo} - \frac{T_{IN} + T_{OUT}}{2}$$

A desired ten degree Celsius difference between the inlet and outlet temperatures required an average wall temperature of forty-five degrees Celsius. Taking into consideration the possible losses in the system, the required power to achieve that average wall temperature was estimated to be a maximum of 40 Watts.

Upon completion of a series of preliminary experiments it was established that a combination of liquid crystals would be required to adequately delineate the average wall temperature and the vortex phenomenon. The test sections were therefore sprayed with a mixture of three NCR Microencapsulated Liquid Crystals (R-41, R-45 and R-49) prepared in accordance with reference 30. Using an artist's air brush, approximately twenty coats of the liquid crystal mixture were applied directly to the Temsheet in order to ensure a sharp color contrast and definition within the response curve of each liquid crystal. It was hoped that the resultant color patterns could be recorded photographically.

A total of sixty-four copper-constantan, glass insulated, 30 gauge thermocouples were constructed and placed in specific locations to measure the required temperatures. All thermocouples were permanently wired to a Hewlett-Packard Data Acquisition System, Model 2010C, which provided an automatic printed record of the instantaneous data for each thermocouple position. The full set of thermocouples were connected in series to a Kaye Instruments Ice Point Reference, Model K-140-4. In each test section five thermocouples were inserted between the first and second layers of the insulation with an additional five inserted between the second and third layers. Each set of five thermocouples were connected in parallel to read an averaged temperature value (T_{INS}) between

the respective insulation layers. A set of four thermocouples, also connected in parallel, were inserted into the flow channel at each of the following locations: the entrance to the channel, the exit of the straight test section, and the exit of the curved test section. At each location the thermocouples were distributed in a spanwise interval of 5.0 cm and at a depth of 0.3 cm to allow the thermocouples to read a bulk temperature for the air flow. In each test section eight thermocouples were placed in direct contact with the Temsheet through very small diameter holes drilled in the Plexiglas above the Temsheet and the thermocouple beads were electrically insulated from the Temsheet with ENMAR Heat Resisting Glyceryl Phthalate. An additional eight thermocouple beads were embedded in the Plexiglas channel opposite those positioned in the Temsheet. Figure 6 provides a detailed sketch of this thermocouple arrangement. The thermocouples in contact with the Temsheet provided an average outer wall temperature (T_{wo}) and confirmed temperature distributions indicated by the liquid crystal patterns. Those in the Plexiglas channel wall provided an average inner wall temperature (T_{wi}) and assisted in estimating the losses in the system due to radiation. All the thermocouples were calibrated using a ROSEMOUNT Communtating Bridge, model 920A, and a ROSEMOUNT Constant Temperature Bath, Model 913A.

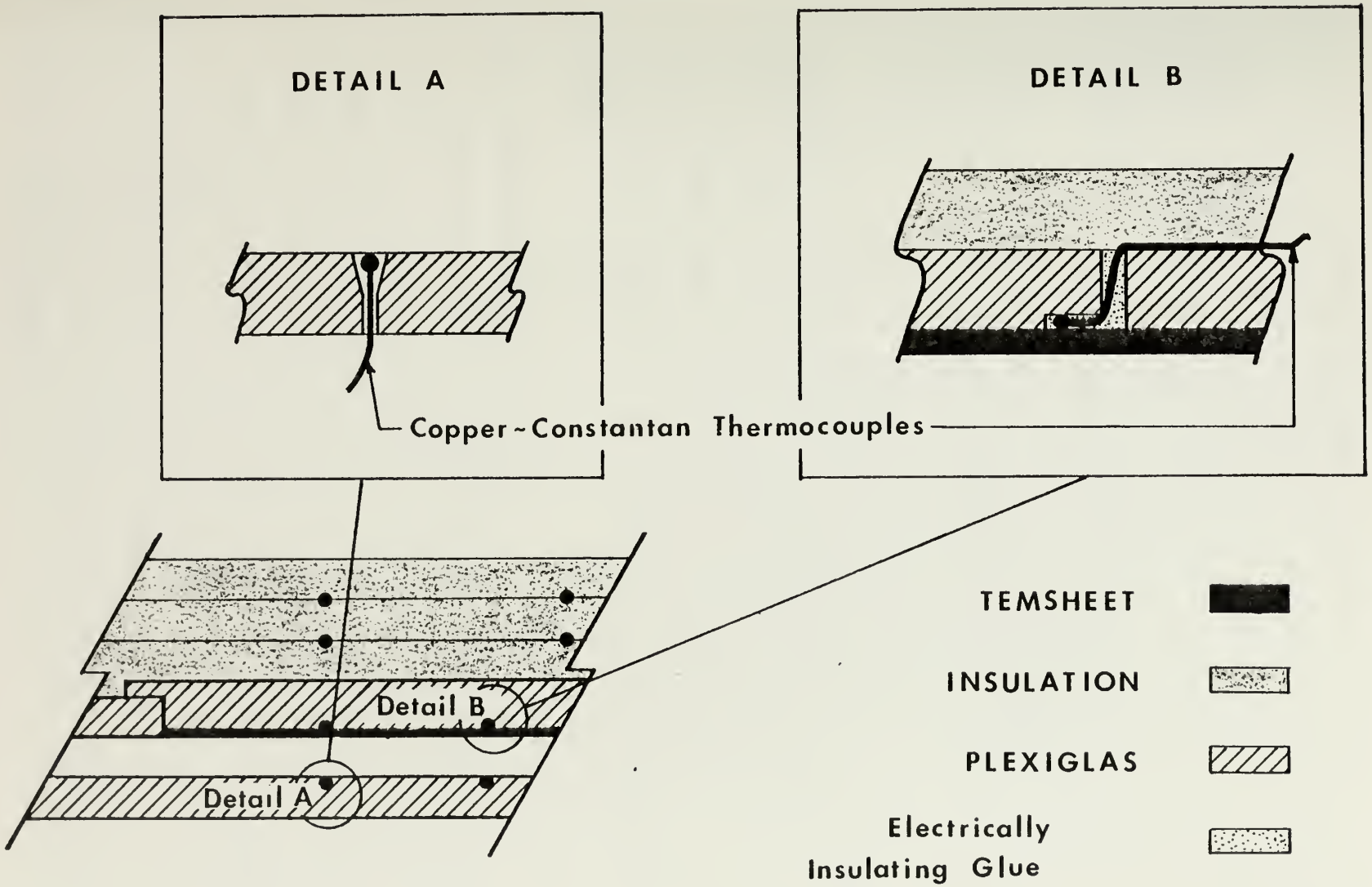

Figure 6. Location of Thermocouples in Test Sections

The thermal insulation consisted of Armstrong ARMAFLEX 22 Sheet Insulation which is a flexible foam plastic material. Three layers of insulation were used, each one with a thickness of 0.635 cm and covering an area slightly larger than each test section. The insulation was fixed in place with the use of an Adhesive Heat Resistant Ventilation Duct Tape as shown in Figure 7. The entire length of the channel was sealed with GENERAL ELECTRIC Silicone Rubber sealant caulk.

Two aluminum electrodes, 0.318 cm thick, were inserted between the Temsheet and the Plexiglas as shown in Figure 3. Each plate consisting of the Temsheet, the liquid crystals, the thermocouples and the aluminum electrodes was affixed in the channel using Teflon screws to provide electrical insulation.

B. EXPERIMENTAL PROCEDURES

Experiments were conducted for each test section following the same set of procedures. The data obtained in the straight test section provided baseline information for later curved section runs, either aligned with or opposed to the buoyancy forces. The volumetric flow rate was varied incrementally from 0.063 to 0.220 cubic meters of air per minute to correspond to values of Reynolds numbers in the laminar flow regime. Data was recorded and calculations were performed for each flow rate increment.

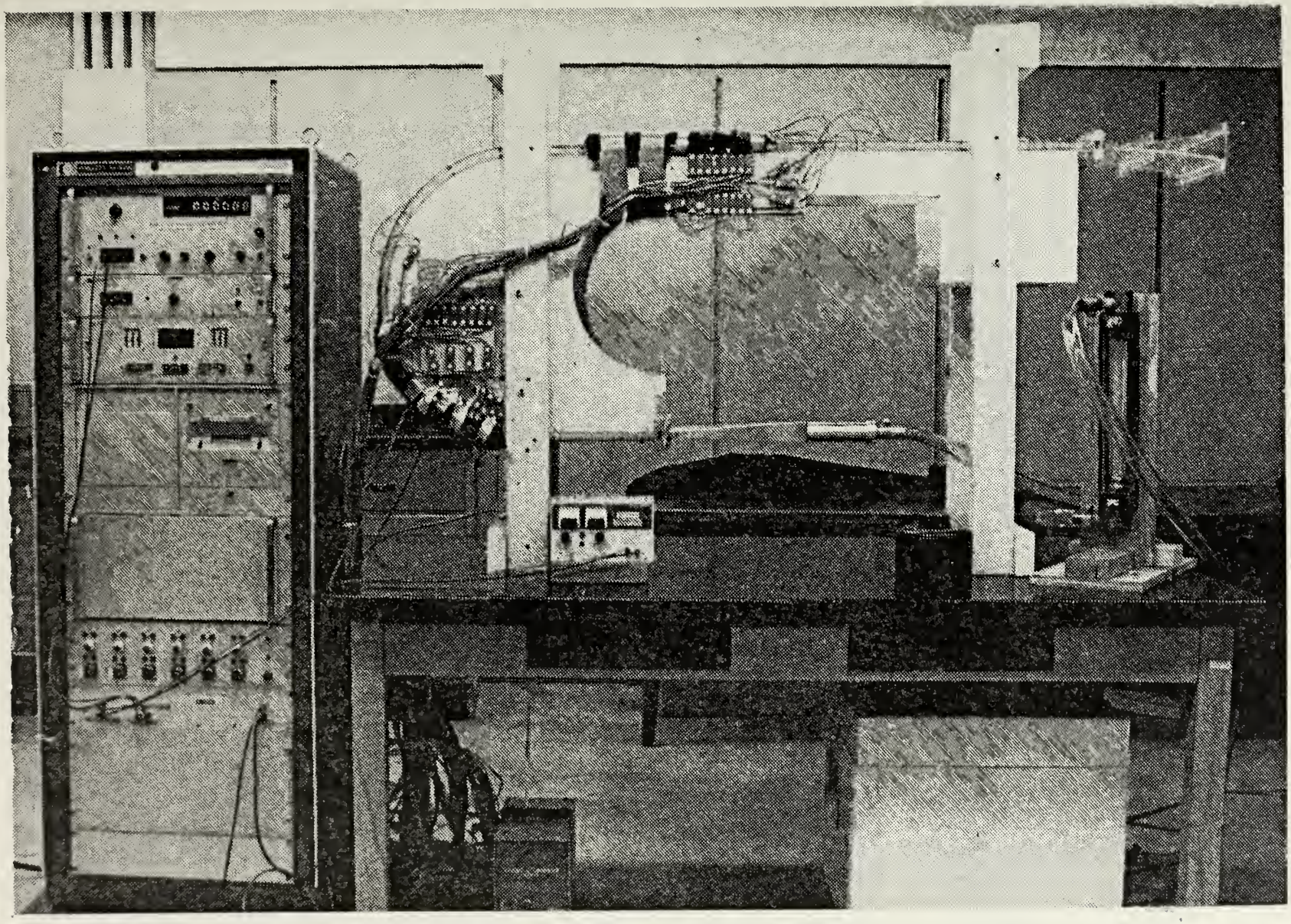

Figure 7. General Arrangement of Apparatus and Instrumentation

The appropriate electrical power required to heat the Temsheet to a temperature level that would initiate the liquid crystal response was determined through preliminary experiments.

Estimates of the time required for the experiment to reach steady state, decisions on what data would be recorded, and frequencies at which that data would be obtained were also based on preliminary runs.

The determination as to what constituted a steady-state condition required careful consideration in light of the influence that the multiple input variables could have on the results. The final criteria for steady-state was based on three input variables; the flow rate percentage, the outside wall temperature (Temsheet), and the heater voltage. When these input conditions had a variation of less than two percent over a ten minute interval, the experiment was considered to have reached steady-state. Under these guidelines the assumptions of steady flow and constant heat flux from the upper wall were valid.

The time required to reach steady-state was found to be between two and two and one-half hours. Accordingly, all runs were two and one-half hours in duration. Data was recorded at one hour intervals for the first two hours and at ten minute intervals thereafter.

The instantaneous values for all the temperatures were automatically printed by the digital recorder in milivolts. A standard thermocouple table was used in conjunction with previously obtained thermocouple calibration data to convert the milivolts to degrees Celsius. The volumetric flow rate was read directly from the rotameter. The precision resistor voltage (V_{PR}) and the heater voltage (V_H) were recorded in volts and the instantaneous voltage supplied (Q_p) was calculated using the following relationship:

$$Q_p = \frac{V_{PR}\, V_H}{R_{PR}}$$

where R_{PR} was 2.0236 ohms, the measured electrical resistance of the precision resistor in the circuit.

The steady state response of the liquid crystals was recorded photographically using a NIKOMAT (FTN) 35mm single reflex camera with a 85 - 205 mm zoom lens. The film was 25 ASA Kodachrome with the shutter speed and lighting controlled manually.

All data reduction was accomplished by desk-top computer programs and stored routines.

IV. PRESENTATION OF DATA

A. ANALYSIS

The flow examined in this study was laminar and steady, thus in a general sense, plane Poiseuille flow. The Temsheet which possessed the property of uniform electrical resistivity approximated a constant axial and peripheral wall heat flux. Temperature measurements on the Plexiglas wall opposite the heated surface indicated negligible heat loss through that wall, i.e., adiabatic. With an aspect ratio of 40 the channel was approximated by infinite parallel plates. The straight portion of the flow channel, upstream from the straight test section, was of sufficient length to ensure that the flow was hydrodynamically developed for all flow velocities in the laminar range. For the purposes of this study, the flow was considered laminar when the value of the Reynolds number was less than 2000. Based on the above assumptions, the experimental configuration was then modeled as laminar forced convection between parallel plates with hydrodynamically developed and thermally developing flow. The boundary conditions are fundamental boundary conditions of the second kind with one wall at a specified axial and peripheral heat flux and the other wall insulated. [28]

The appropriate variables, corresponding equations and solution procedures are contained in the following paragraphs.

The average heat transfer coefficient from the heated wall to the flow of air was defined by a form of Newton's law of cooling:

$$Q_{air} = \bar{h} A_{PL} \Delta T$$

In this expression, Q_{air} was the heat convected to the air, $\bar{h}$ was the average heat transfer coefficient, A_{PL} was the surface area of the heated Temsheet, and ΔT was the temperature difference between the average wall temperature (T_{wo}) and the bulk temperature of the fluid (T_B).

The actual heat convected to the air (Q_{air}) was then independently calculated with the equation:

$$Q_{air} = \dot{m} C_{pair} (T_{OUT} - T_{IN})$$

where C_{pair} was the specific heat of air at constant pressure and $\dot{m}$ was the mass flow rate of the air. The mass flow rate was the product of the volumetric flow rate ($\dot{q}$) and the local flow density in the rotameter (ρ). The volumetric flow rate was corrected to standard air conditions for the rotameter and the local flow density was calculated assuming perfect gas behavior at constant pressure and using the flow exit temperature (T_{EXIT}).

The average Nusselt number was determined from the average heat transfer coefficient using the following expression:

$$\overline{Nu} = \frac{\bar{h}d}{K_{air}}$$

where d represented the height of the channel and K_{air} was the thermal conductivity of the air evaluated at the bulk temperature (T_B).

The Reynolds number was calculated for all the experimental runs and was defined as:

$$Re = \frac{\rho u d}{r} = \frac{\dot{m}d}{\mu A_c}$$

where d was the height of the channel, μ was the dynamic viscosity of the air at the flow exit temperature and A_c was the cross sectional area of the channel.

For all experiments in the curved test section, the Dean number was calculated as:

$$De = Re \sqrt{\frac{d}{Ri}}$$

In this equation d was again the height of the channel and Ri was the radius of curvature of the inner convex wall.

To verify that Q_{air}, which was indirectly measured by the temperature rise across the channel, was actually the convection heat transfer from the heated Temsheet surface, an estimate of the radiation heat transfer was made for each run. The average temperature of the lower plate was measured by

eight thermocouples and the radiated heat transfer (Q_r) was calculated with the Stefan-Boltzman law of radiation:

$$Q_r = \frac{\sigma(T_{wo}^4 - T_{wi}^4)}{R_R}$$

where σ is the Stefan-Boltzman constant and R_R represents the total resistance to radiation heat transfer between the plates as given by:

$$R_R = \frac{1}{A_{PL}} \left[\frac{1}{\varepsilon_{wo}} + \frac{1}{\varepsilon_{wi}} - 1 \right]$$

In this form ε_{wo} represented the emissivity of the heated Temsheet surface and ε_{wi} was the emissivity of the adiabatic Plexiglas surface.

Appendix B contains a representative heat balance and sample calculations for one of the experimental runs.

B. RESULTS

Utilizing the expressions described earlier, the experimental data for buoyant forces aligned with the main direction of the fluid flow was reduced in accordance with the sample calculation procedure shown in Appendix B. Results for the major variables involved are provided in tabular and graphical form on the following pages. Table I and II show computed values for the straight and the curved test sections respectively. Figure 8 contains a plot comparing the average Nusselt number versus the Reynolds number for both test

sections. Representative uncertainty bands have been indicated for all plotted experimental data and a complete error analysis is provided in Appendix A.

TABLE I

SUMMARY OF RESULTS FOR STRAIGHT TEST SECTION

Re	$h(W/m^2{}^\circ C)$	$\overline{Nu}$
989	22.51	5.321
876	22.21	5.298
826	21.79	5.198
751	21.75	5.197
689	20.72	4.941
632	20.95	4.897
560	19.20	4.559
488	18.79	4.482
438	17.75	4.234
363	16.99	4.053
313	16.24	3.874
263	14.30	3.512

TABLE II

SUMMARY OF RESULTS FOR CURVED TEST SECTION

Re	Dc	$\bar{h}$(W/m^2°C)	$\overline{Nu}$
990	144	27.81	6.694
865	126	27.74	6.617
803	117	25.06	5.977
741	108	23.42	5.588
678	99	22.57	5.384
654	95	22.43	5.351
616	90	22.07	5.265
579	84	21.67	5.169
554	81	21.34	5.091
523	76	20.58	4.875
492	72	20.28	4.838
429	63	20.20	4.819
404	59	20.31	4.844
367	54	18.95	4.515
342	50	17.76	4.236
306	45	15.76	3.759
274	40	14.50	3.460
244	36	13.12	3.130

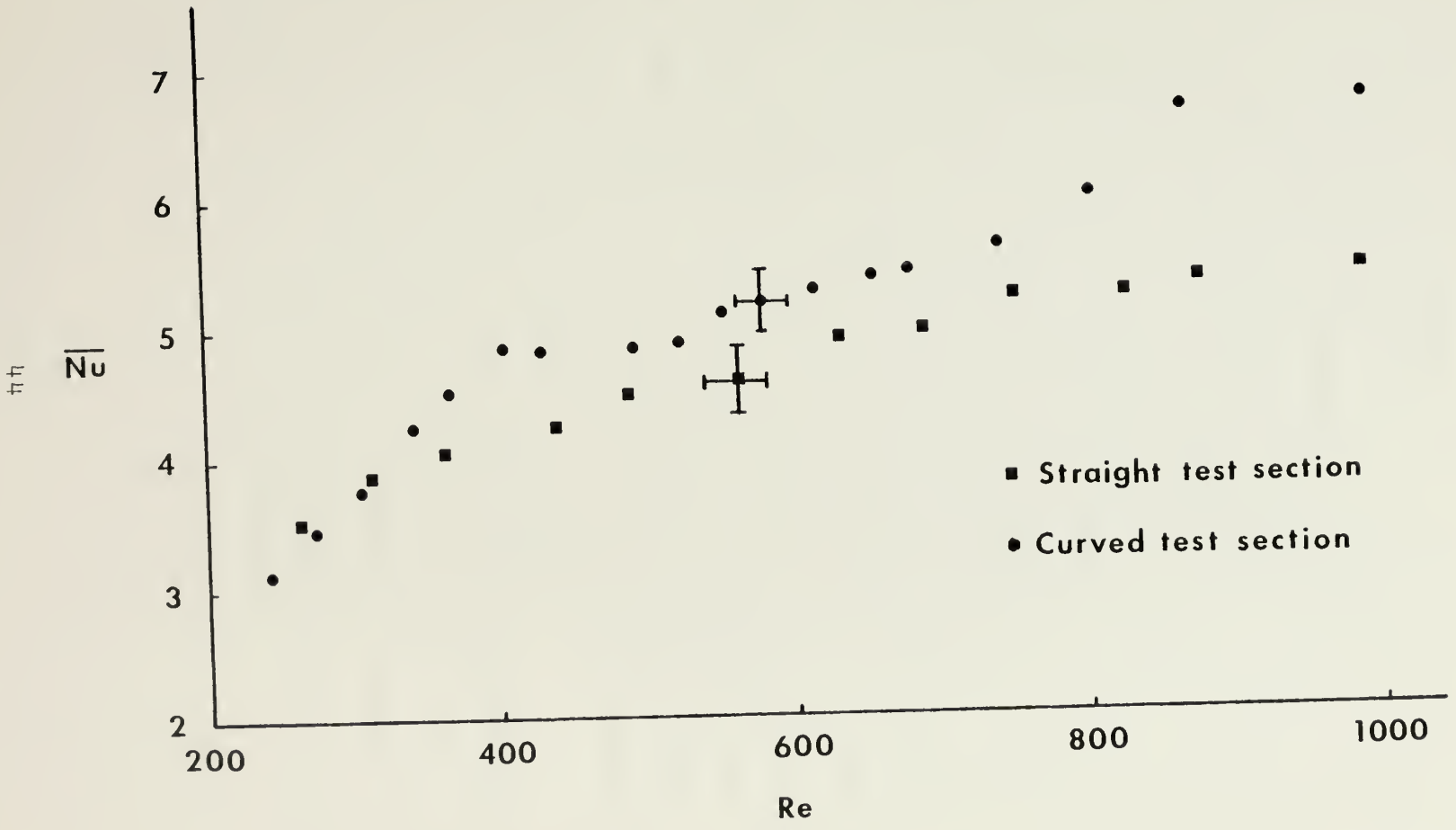

Figure 8. Average Nusselt Number versus Reynolds Number for Both Test Sections

In all cases the results indicated an increase in the heat transfer rates as the flow velocity, i.e., Reynolds number, was increased. However, when comparing the average Nusselt numbers of the straight and curved sections two distinct regions became evident. At the highest values of Reynolds number, which corresponded to the highest volumetric flow rates, it was observed that the values of the average Nusselt number for the curved test section were greater than those in the straight test section. At the low and intermediate values of Reynolds number, the data was less conclusive with regards to the comparative values of the average Nusselt number in each test section. This region, between Reynolds numbers of 200 and 400, corresponded to values of the Dean number between 30 and 60. As Dean discussed in his work concerning flow instability in a curved channel [12], a small disturbance would not be amplified below the critical Dean value of 36. Above this critical value, his linearized prediction indicated the disturbance would increasingly amplify as flow velocity increased.

Consequently, it was concluded that the Taylor-Görtler vortices are only initially developing in the low to intermediate Reynolds number region and have not yet reached sufficient proportion to have any significant effect on the heat transfer rates in the curved section.

The actual presence and onset of the Taylor-Görtler vortices was independently verified through the observation of the liquid crystal isotherm distribution on the Temsheet surface in the curved test section. At the smallest values of Reynolds number, the liquid crystals were in essentially straight bands that were perpendicular to the flow direction (Figure 9). A similar pattern was observed in the straight test section for the entire experimental range of Reynolds numbers. This pattern was thought to indicate that the flow was in essence two-dimensional. As the value of the Reynolds number was increased, liquid crystal bands orientated in the streamwise directions became visible at the trailing edge of the curved test section. At the onset of these streamwise bands the liquid crystal bands at the leading edge remained orientated perpendicular to the flow direction. As the Reynolds number was further increased, the bands which were orientated in the streamwise direction eventually became evident over the entire surface of the curved test section (Figure 10). These streamwise bands would indicate a transition from the initial, stable, two-dimensional flow to a less stable, three-dimensional flow triggered by the continuing development of the Taylor-Görtler vortices.

The simultaneous occurrence of the streamwise bands, explained by the presence of the longitudinal Taylor-Görtler vortices, and the increase in the average Nusselt number

Figure 9. Distribution of Liquid Crystal Color Bands in Curved Test Section for Re=250 (De=35)

Figure 10. Distribution of Liquid Crystal Color Bands in Curved Test Section for Re=800 (De=117)

justified the conclusion that the vortices did in fact enhance heat transfer from the curved test section.

Comparison of the average Nusselt numbers for the straight and curved test section indicated that values for the ratio of Nu_c to Nu_s could be separated into two categories. For Reynolds numbers between 400 and 800, the heat transfer rate was increased by an average of eleven percent. For Reynolds numbers above 800, the heat transfer rate was increased by more than twenty-five percent. In an earlier investigation of the boundary layer along a concave wall, Kreith [4], reported that heat transfer rates along concave walls increased from twenty-five percent to sixty percent for Reynolds numbers, based on the hydraulic diameter, between 10^4 and 10^6. This would suggest that the two data points for Reynolds numbers greater than 800 in the curved test section could represent flow that has tripped and become turbulent, or at least entered a laminar-turbulent transition. One possible explanation could be that the Taylor-Görtler vortices have started to break down at this point and have therefore initiated transition to the turbulent flow regime.

Experimental data obtained for the curved test section with the buoyant forces opposed to the main direction of the flow indicated a minimal difference in heat transfer rates from the curved channel. This small decrease was only

evident at very low volumetric flow rates and became negligible for Reynolds numbers greater than 500.

V. DISCUSSIONS AND CONCLUSIONS

Investigation of the measured wall and air flow temperatures indicated there was negligible difference between the unheated wall temperature and the fluid bulk temperature. In addition, energy balances such as the one detailed in Appendix B provided evidence that the radiation heat transfer from the unheated wall was minimal. Based on this information, it was assumed that the heat convected to the air flow was solely from the heated wall.

As previously discussed, the high aspect ratio of the channel provided the basis from which the initial assumption was made to model the experimental apparatus configuration as infinite parallel plates. The experimental data was found to substantiate this assumption as the computed values of the average Nusselt number in the straight section asymptotically approached the theoretical value of 5.385 for parallel plates with one wall at a constant heat flux and the opposite wall adiabatic. [28]

With the formulation of the problem complete, the experimental data could now be compared with analytical solutions of the same problem; i.e., laminar flow between infinite parallel plates with one wall at constant heat flux and the opposite wall adiabatic. In particular, the experimental

results were compared with two analytic studies; one conducted by McCuen, et al.[26], for infinite parallel plates, and the other conducted by Worsøe-Schmidt [27] for tubes and annular passages. In the case of the annular passages the results were compared to the numerical predictions for an annulus with an infinite inner and outer radius of curvature, thereby approximating parallel plates.

Before comparing the experimental data with the studies mentioned above, it would be advantageous to address the initial assumptions and review the nomenclature common to both those studies. First, the following restrictions are applied in the mathematical formulation of the problem:

1. the velocity profile is fully established
2. the fluid transport properties and density are assumed constant
3. axial heat conduction is negligible
4. viscous energy dissipation is negligible
5. conditions are invariant with time (steady state)

All of these restrictions have been accounted for in the design of the experimental configuration and/or verified in the experimental process. Next, a dimensionless axial length coordinate was defined as follows:

$$x^* = \frac{x}{D_h \, Pr \, Re}$$

where x was the length of the straight test section (29.2 cm), Dh was the calculated hydraulic diameter (1.239 cm), and Pr was the Prandtl number (0.70). In these studies, the Reynolds number (Re) was calculated on the basis of the hydraulic diameter. The values of x* indicated that the development of the experiments would most likely occur in the thermal entrance region. Analysis of the temperature distribution on the heated wall versus the axial length verified the flow was indeed thermally developing.

In comparing the experimental results to those reported by McCuen, et al., it was necessary to integrate their expression of the local Nusselt number for small values of x*;

$$Nu = \frac{1}{0.67095\ x^{*1/3} - 2\left(1 + \frac{Q_{wi}}{Q_{wo}}\right)x^*}$$

in order to obtain the following expression for the average Nusselt number.

$$\overline{Nu} = \frac{-3}{4\left(1+\frac{Q_{wi}}{Q_{wo}}\right)x^*} \ln\left[1 - \frac{2}{0.67095}\left(1 + \frac{Q_{wi}}{Q_{wo}}\right)x^{*2/3}\right]$$

In this expression Q_{wi} would represent the heat convected to the air from the inner Plexiglas wall and Q_{wo} would be the heat convected from the outer Temsheet wall. The average Nusselt number was then calculated in accordance with the

experimental model where Q_{wi} was equal to zero and Q_{wo} was synonymous with Q_{air}.

The experimental data obtained for the straight section was then recalculated as a function of the hydraulic diameter and both the experimental and analytical results were plotted in Figure 11. Note that the analytic expression for the average Nusselt number was only plotted for values of the Reynolds number that corresponded to x* less than 0.042 as this represented the maximum value for which the analytic solutions would be valid. Neglecting those experimental data points that plotted outside this valid range, there was good agreement between the experimental and the analytic results.

A similar process was followed to compare the experimental results with those reported by Worsøe-Schmidt. Again the analytic values for the local Nusselt number were integrated to obtain analytic values for the average Nusselt number. In this case the experimental and analytic values of average Nusselt number were plotted versus the non-dimensional axial length coordinate x*. The results are shown in Figure 12. Similarly, there was good agreement between the experimental and the analytic results.

It is noted that in both cases where the analytic and experimental results were compared, the experimental data plotted above the analytic predictions. This difference can be explained, at least in part, by the limitations that are

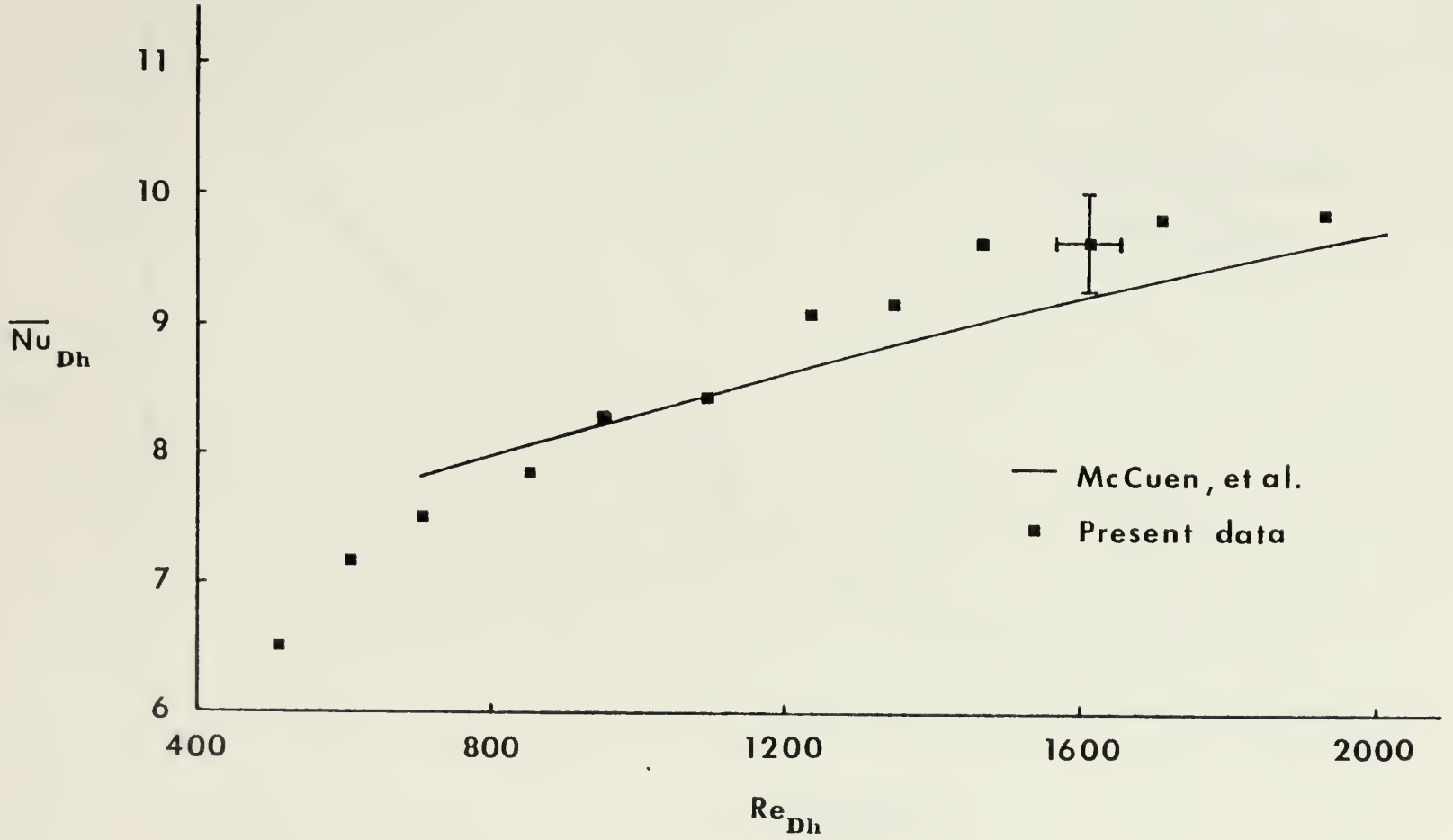

Figure 11. Comparison of Present Results with the Study by McCuen, et al.

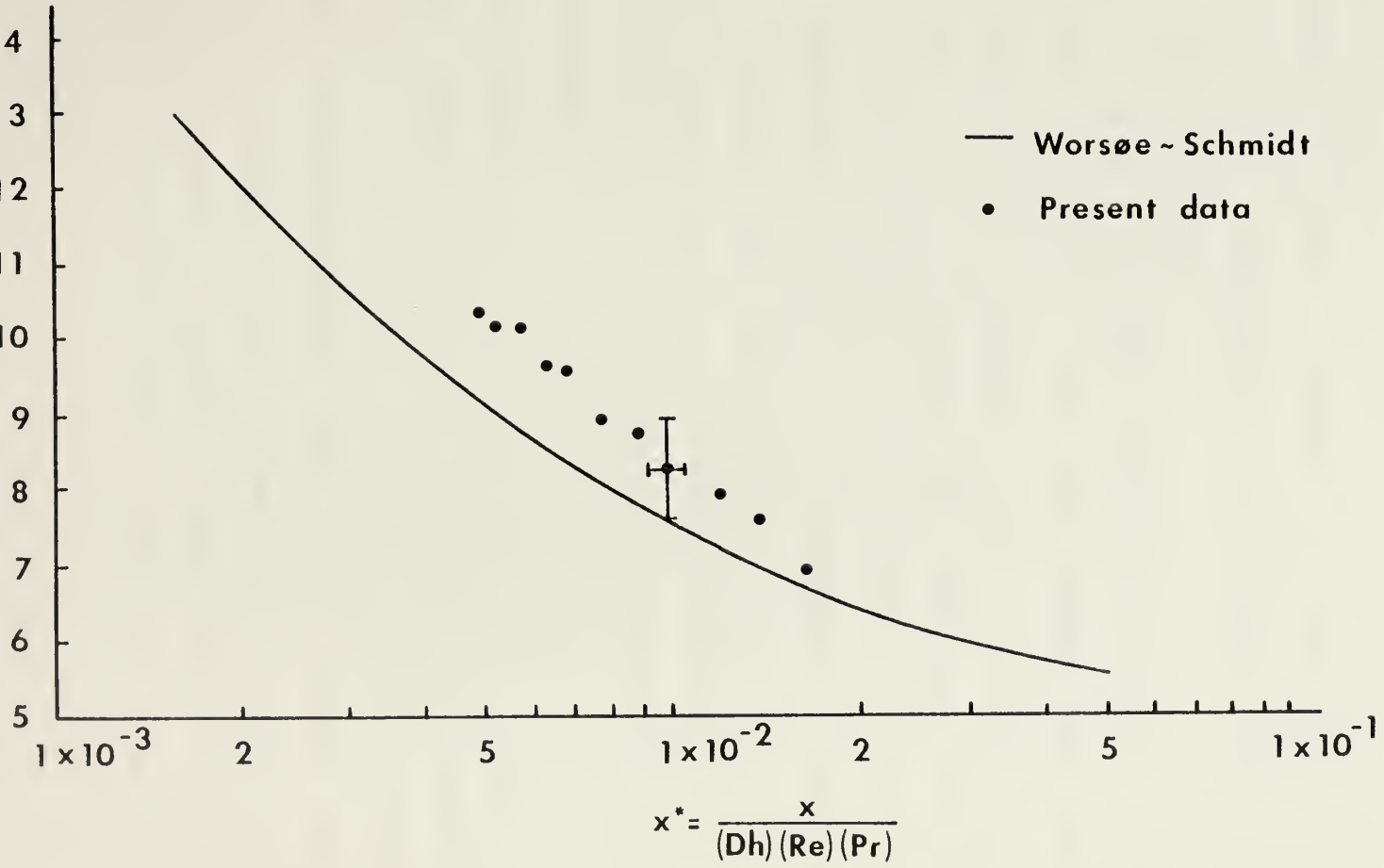

Figure 12. Comparison of Present Results with the Study by Worsøe-Schmidt

inherent in any experimental configuration. In this case, the presence of side wall effects and the inability to totally account for all the heat transfer processes and/or losses combine to produce a slightly inflated value of the heat transfer rate. Consequently, the average Nusselt number is also slightly inflated.

Irrespective of the slight differences locally, the overall trends were conclusive. The heat transfer rates were shown to increase with increasing values of Reynold number. The ratio of N_{uc} to N_{us} indicated that there was a measureable increase in the heat transfer rate from the curved section once the Taylor-Görtler vortices had developed to sufficient strength. Although much less conclusive from this experimental data, it appeared the the Taylor-Görtler vortices were additionally important in the transition from laminar to turbulent flow.

The experimental data from the curved test section when the buoyant forces were opposed to the main flow direction was essentially inconclusive. While the trend was qualitatively what had been expected, that is, the average Nusselt number for the buoyant forces aligned with the flow was greater than that for the buoyant forces opposed to the flow; the difference was insignificant in light of the experimental uncertainties.

VI. RECOMMENDATIONS

While the amount of work remaining in the experimental study of heat transfer in a curved channel has been reduced for laminar flows, a large amount still remains to be accomplished. Additional experiments should be conducted to refine the correlation for the average Nusselt number as a function of the Dean number. Further work should certainly be considered in the region where the laminar flow begins its transition to turbulent flow. Detailed study in this area could provide important data to determine the manner of relationship that exists between Taylor-Görtler vortices and laminar-turbulent transition. With this work it will be necessary to design and construct a larger experimental configuration capable of higher volumetric flow rates and increased ΔT through the test sections.

Finally it would be advantageous to do more experimental work in the general area of liquid crystal thermography, and more specifically, the photography of these crystals and their distribution.

APPENDIX A

ERROR ANALYSIS

The uncertainties for the major variables in the experiments were calculated in accordance with the method described by S. Kline and F. McClintoch [31]. The estimates of the uncertainty in the measured quantities were made conservatively so that there was considerable confidence in the calculated uncertainties. As an example, the calculation of the uncertainty for the Reynolds number is given below. The Reynolds number was defined by the equation:

$$Re = \frac{\dot{m}d}{\mu_{air} A_c}$$

and the uncertainty was calculated as:

$$\frac{dRe}{Re} = \sqrt{(\frac{d\dot{m}}{\dot{m}})^2 + (\frac{dd}{d})^2 + (\frac{d\mu_{air}}{\mu_{air}})^2 + (\frac{dA_c}{A_c})^2}$$

The uncertainty in the mass flow rate was determined as follows:

$$\frac{d\dot{m}}{\dot{m}} = \sqrt{(\frac{dP}{P})^2 + (\frac{dR}{R})^2 + (\frac{dT}{T})^2 + (\frac{dQ}{Q})^2}$$

The uncertainty in the pressure, the gas constant, the temperature, the reading of the volumetric flow rate, the height of the channel, the dynamic viscosity and the cross

sectional area of the channel were obtained from estimates as follows:

$$\frac{dP}{P} = 0.00048,\ \frac{dR}{R} = 0.00002,\ \frac{dT}{T} = 0.00056,\ \frac{dQ}{Q} = 0.02000,$$

$$\frac{dd}{d} = 0.02003,\ \frac{d\mu_{air}}{\mu_{air}} = 0.00223,\ \text{and}\ \frac{d\,A_c}{A_c} = 0.02054.$$

The uncertainty in the mass flow rate was:

$$\frac{d\dot{m}}{\dot{m}} = \sqrt{(0.00048)^2+(0.00002)^2+(0.00056)^2+(0.02000)^2} = 0.02001$$

and the uncertainty in the Reynolds number could then be calculated as:

$$\frac{dRe}{Re} = \sqrt{(0.02001)^2+(0.02003)^2+(0.00223)^2+(0.02054)^2} = 0.03505$$

The values of the uncertainties for all variables are listed below:

Quantity	Uncertainty
A_c	0.02054
A_{PL}	0.00266
C_{pair}	0.00415
De	0.04042
$\bar{h}$	0.02149
K_{air}	0.00038
$\overline{Nu}$	0.02938

Quantity	Uncertainty
$\dot{m}$	0.02001
Q	0.02000
Q_{air}	0.03548
R_e	0.03505
T_B	0.00482
T_{IN}	0.00257
T_{OUT}	0.00950
T_w	0.00583
$T_{OUT}-T_{IN}$	0.02900
$\Delta T=T_W-T_B$	0.00736
μ	0.00223
ρ	0.00074

APPENDIX B

SAMPLE CALCULATIONS

Figure 13 provides a representation of the control volume used in the energy balance on the straight test section. The sample calculations that follow indicate the procedure used to obtain the heat transfer components required for the energy balance and eventually the values of the average Nusselt number as a function of the Reynolds number for the air flow. A similar energy balance and procedure was used for the curved test section.

ENERGY BALANCE

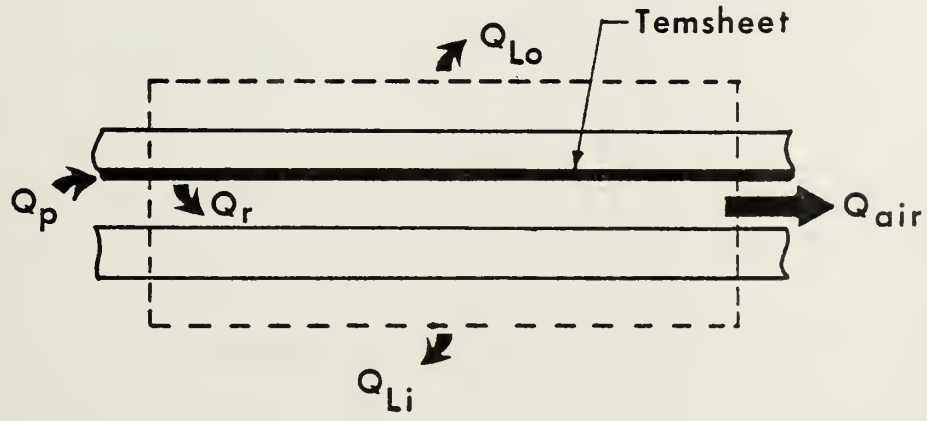

Figure 13. Energy Balance in the Straight Test Section

SAMPLE CALCULATIONS

A. DATA

T_{ROOM} = 23.0°C

Q = 45%

V_{PR} = 2.583 V

V_u = 30.008 V

R_{PR} = 2.024 Ω

T_{IN} = 0.892 mV = 23.07 °C

T_{INS1} = 1.597 mV = 39.54 °C

T_{INS2} = 1.339 mV = 33.45 °C

Two1 = 1.853 mV

Two2 = 1.843 mV

Two3 = 2.010 mV

Two4 = 2.014 mV

Two5 = 2.144 mV

Two6 = 2.141 mV

Two7 = 2.274 mV

Two8 = 2.239 mV

Two = 50.47 °C

Twi1 = 1.079 mV

Twi2 = 1.083 mV

Twi3 = 1.130 mV

Twi4 = 1.131 mV

Twi5 = 1.183 mV

Twi6 = 1.172 mV

Twi = 28.62 °C

T_{wi7} = 1.219 mV

T_{wi8} = 1.216 mV

T_{OUT} = 1.383 mV = 34.09 °C

T_{EXIT} = 0.934 mV = 23.53 °C = 74.35 °F

A_{PL} = 0.0742 m^2

A_c = 0.0016 m^2

d = 0.00635 m

K_{air} = 0.02662 w/m °C

Cp_{air} = 1.0057 KJ/Kg °C

μ_{air} = 1.983 x 10^{-5} Kg/m·sec

K_{INS} = 4.18 x 10^{-2} W/m °C

ΔX_{INS} = 0.00635 m

ε_{wo} = 0.70

ε_{wi} = 0.40

F_{wo-wi} = 1.0

σ = 5.669 x 10^{-8} W/m^2 °K

B. TEMPERATURE CALCULATIONS

1. Temperature Difference in Insulation (ΔT_{INS})

$\Delta T_{INS} = T_{INS1} - T_{INS2} = 39.54 - 33.45 = 6.09$ °C

2. Bulk Temperature (T_B)

$$T_B = \frac{T_{IN} + T_{OUT}}{2} = \frac{23.07 + 34.09}{2} = 28.58 \text{ °C}$$

3. Mean Temperature Difference (ΔT)

$\Delta T = T_{wo} - T_B = 50.47 - 28.58 = 21.89$ °C

C. POWER CALCULATIONS

1. Power Supplied (Q_P)

$$Q_P = \frac{V_{PR}\, V_H}{R_{PR}} = \frac{(2.583)(30.008)}{(2.024)} = 38.30 \text{ W}$$

2. Heat Lost Through Outer Plate (Q_{Lo})

$$Q_{Lo} = \frac{\Delta T_{INS}}{\Delta X_{INS}/K_{INS} \cdot A_{PL}} = \frac{6.09}{(0.00635)/((4.18\text{x}10^{-2})(0.0742))}$$

$$= 2.97 \text{ W}$$

3. Heat Radiated (Q_r)

a. Radiation Resistance (R_R)

$$R_R = \frac{1-\varepsilon_{wo}}{A_{PL}\varepsilon_{wo}} + \frac{1}{A_{PL}\, F_{wo-wi}} + \frac{1-\varepsilon_{wi}}{A_{PL}\, \varepsilon_{wi}}$$

$$= \frac{1}{A_{PL}} \left[\frac{1}{\varepsilon_{wo}} + \frac{1}{\varepsilon_{wi}} - 1\right] = \frac{2.929}{A_{PL}}$$

b. Heat Radiated (Qr)

$$Qr = \frac{\sigma(T_{wo}^{\,4} - T_{wi}^{\,4})}{R_R} \qquad T \equiv {}^\circ K$$

$$= \frac{(5.669\text{x}10^{-8})(0.0742)(323.63^4 - 301.78^4)}{2.929}$$

$$= 3.843 \text{ W}$$

4. Heat Convected to Air (Q_{air})

a. Corrected Volumetric Flow Rate ($\dot{q}$)

$$\dot{q} = Q\sqrt{\Theta} = Q\sqrt{\frac{T_{EXIT}\ (°R)}{T_{STANDARD}\ (°R)}}$$

$$= \frac{(0.314)(0.45)}{60} \sqrt{\frac{534.04}{529.69}}$$

$$= 0.0024\ m^3/sec$$

b. Density (ρ)

$$\rho = \frac{P}{R\ T_{EXIT}} = \frac{1.013 \times 10^5}{(287)(23.53+273.16)}$$

$$= 1.189\ Kg/m^3$$

c. Mass Flow Rate ($\dot{m}$)

$$\dot{m} = \dot{q}\rho = (0.0024)(1.189) = 0.0028\ Kg/sec$$

d. Heat Convected to Air (Q_{air})

$$Q_{air} = \dot{m}\ Cpair\ (T_{OUT}-T_{IN})$$
$$= (0.0028)(1.0057)(34.09-23.07)$$
$$= 0.03103\ KJ/sec$$
$$= 31.03\ W$$

D. AVERAGE HEAT TRANSFER COEFFICIENT ($\bar{h}$)

$$\bar{h} = \frac{Q_{air}}{A_{PL}\,\Delta T} = \frac{31.03}{(0.0742)(21.89)}$$

$$= 19.11\ W/M^2{}^\circ C$$

E. AVERAGE NUSSELT NUMBER ($\overline{Nu}$)

$$\overline{Nu} = \frac{\bar{h}d}{Kair} = \frac{(19.11)(0.00635)}{(0.02662)} = 4.559$$

F. REYNOLDS NUMBER (Re)

$$Re = \frac{\dot{m}\,d}{\mu_{air}\,A_c} = \frac{(0.0028)(0.00635)}{(1.983x10^{-5})(0.0016)}$$

$$= 560.39$$

$$= 560$$

LIST OF REFERENCES

1. Taylor, G.I., "Stability of a Viscous Liquid Contained Between Two Rotating Cylinders", Philosophical Transactions of the Royal Society of London, series A, V.223, pp. 289-343, 1923.

2. National Advisory Committee for Aeronautics, Technical Memorandum 1375, On the Three Dimensional Instability of Laminar Boundary Layers on Concave Walls, by H. Görtler, 1942.

3. Smith, A.M.O., "On the Growth of Taylor-Görtler Vortices Along Highly Concave Walls", Quarterly of Applied Mathematics, V.8, pp. 233-262, November 1955.

4. Kreith, F., "The Influence of Curvature on Heat Transfer to Incompressible Fluids", Trans. ASME, V.77, pp. 1247-1256, 1955.

5. Mori, Y., and Uchida, Y., "Forced Convective Heat Transfer Between Horizontal Flat Plates", International Journal of Heat and Mass Transfer, V.9, pp. 803-817, 1966.

6. Tobak, M., "Hypothesis for the Origin of Cross-Hatching", AIAA Journal, V.8, No. 2, pp. 330-334, February 1970.

7. Mayle, R.E., Kopper, F.C., Blair, M.F., and Bailey, D.A., "Effect of Streamline Curvature on Film Cooling", Journal of Engineering for Power, Trans. ASME, V.99, Series A, No. 1, pp. 77-82, January 1977.

8. Nicolas, J. and LeMeur, A., "Curvature Effects on a Turbine Blade Cooling Film", ASME Paper No. 74-GT-156.

9. Folayan, C.O. and Whitelaw, J.H., "The Effectiveness of Two-Dimensional Film-Cooling Over Curved Surfaces", ASME Paper No. 76-HT-31.

10. Lord Raleigh, "On the Dynamics of Revolving Fluids", Proceedings of the Royal Society of London, series A, V.93, pp. 148-154, 1916. Reprints in Scientific Papers, V.6, pp. 447-453.

11. Taylor, G.I., "Distribution of Velocity and Temperature Between Concentric Rotating Cylinders", Proceedings of the Royal Society of London, Series A, V.151, pp. 494-512, 1935.

12. Dean, W.R., "Fluid Motion in A Curved Channel", Proceedings of the Royal Society of London, Series A, V.121, pp. 402-420, 1928.

13. Reid, W.H., "On the Stability of Viscous Flow in a Curved Channel", Proceedings of the Royal Society of London, Series A, V.244, pp. 186-198, 1958.

14. Schlichting, H., Boundary Layer Theory, 7th ed., pp. 529-536, McGraw-Hill, 1979.

15. Kelleher, M.D., Flentie, D.L., and McKee, R.J., "An Experimental Study of the Secondary Flow in a Curved Rectangular Channel", Journal of Fluids Engineering, V.102, pp. 92-96, March 1980.

16. Winoto, S.H., Durao, D.F.G., and Crane, R.I., "Measurement Within Görtler Vortices", Journal of Fluids Engineering, V.101, pp. 517-520, December 1979.

17. Aihara, Y., "Nonlinear Analysis of Görtler Vortices", The Physics of Fluids, V.19, pp. 1655-1660, November 1976.

18. Aerospace Research Laboratories Report ARL 65-68, A Simplified Approach to the Influence of Görtler-Type Vortices on the Heat Transfer from a Wall, by Leif N. Persen, May 1965.

19. McCormack, P.D., Welker, H., and Kelleher, M.D., "Taylor-Görtler Vortices and Their Effect on Heat Transfer", Journal of Heat Transfer, V.92, pp. 101-112, February 1970.

20. Kahawita, R. and Meroney, R., "The Influence of Heating on the Stability of Laminar Boundary Layers Along Concave Curved Walls", Journal of Applied Mechanics, V.99, pp. 11-17, March 1977.

21. Akiyama, M., Hwang, G.J., and Cheng, K.C., "Experiments on the Onset of Longitudinal Vortices in Laminar Forced Convection Between Horizontal Plates", Journal of Heat Transfer, V.93, pp. 335-341, November 1971.

22. Cheng, K.C. and Akiyama, M., "Laminar Forced Convection Heat Transfer in Curved Rectangular Channels", International Journal of Heat and Mass Transfer, V.13, pp. 471-490, 1970.

23. Yee, G. and Humphrey, J.A.C., "Developing Laminar Flow and Heat Transfer in Strongly Curved Ducts of Rectangular Cross Section", ASME Paper No. 79-WA/HT-15.

24. Mori, Y., Uchida, Y. and Ukon, T., "Forced Convective Heat Transfer in a Curved Channel with a Square Cross Section", International Journal of Heat and Mass Transfer, V.14, pp. 1787-1805, 1971.

25. Durao, M. do Carmo, Investigation of Heat Transfer in Straight and Curved Rectangular Ducts Using Liquid Crystal Thermography, Eng. Thesis, Naval Postgraduate School, Monterey, California, 1977.

26. Department of Mechanical Engineering, Stanford University, Report No. AHT-3, Heat Transfer with Laminar and Turbulent Flow Between Parallel Planes With Constant and Variable Wall Temperature and Heat Flux, by P.A. McCuen, W.M. Kays, and W.C. Reynolds, 12 April 1962.

27. Worsøe-Schmidt, P.M., "Heat Transfer in the Thermal Entrance Region of Circular Tubes and Annular Passages with Fully Developed Laminar Flow", Internation Journal of Heat and Mass Transfer, V.10, pp. 541-551, 1967.

28. Shah, R.K. and London, A.L., Laminar Flow Forced Convection in Ducts, Supplement 1, pp. 305-312, Academic Press, 1978.

29. Department of Mechanical Engineering, University of California, Berkeley, Numerical Computation of Buoyancy-Induced Recirculation in Curved Duct Laminar Flow, by R. Chilikuri and J.A.C. Humphrey, March 1980.

30. Cooper, T.E., Field, R.J. and Meyer, J.F., "Liquid Crystal Thermography and It's Application to the Study of Convective Heat Transfer", Journal of Heat Transfer, V.97, pp. 442-450, August 1975.

31. Kline, S.J. and McClintock, F.A., "Describing Uncertainties in Single-Sample Experiments", Mechanical Engineering, V.75, pp. 3-8, January 1953.

INITIAL DISTRIBUTION LIST

		No. Copies
1.	Defense Technical Information Center Cameron Station Alexandria, Virginia 22314	2
2.	Library, Code 0142 Naval Postgraduate School Monterey, California 93940	2
3.	Associate Professor M. Kelleher, Code 69Kk Department of Mechanical Engineering Naval Postgraduate School Monterey, California 93940	2
4.	Lieutenant James C. Ballard, III, USN United States Department of Energy Naval Reactors Representative's Office General Delivery Naval Base Branch Post Office Charleston, South Carolina 29408	2
5.	Department of Mechanical Engineering, Code 69 Naval Postgraduate School Monterey, California 93940	1

Thesis 191673
B199 Ballard
c.1 Investigation of heat
transfer in straight and
curved rectangular ducts.